

Measurements of B^0 mesons production cross-section in pp collisions at $\sqrt{s} = 7$ TeV using $B^0 \rightarrow D^{*-} \mu^+ \nu_{\mu} X$ decays

The LHCb Collaboration¹

Abstract

This note presents the measurement of the B^0 meson production cross-section in pp collisions at $\sqrt{s} = 7$ TeV using semi-leptonic decays reconstructed in the channel $B^0 \rightarrow D^{*-} \mu^+ \nu_{\mu} X$. The measurement is performed with data collected with the LHCb detector at the LHC in the pseudorapidity interval $2 < \eta < 6$ using an integrated luminosity of 14.9 nb^{-1} .

¹Conference note prepared for the 35th International Conference on High Energy Physics (ICHEP), Paris, 22-28 July 2010; contact authors Marta Calvi, Stefania Vecchi.

1 Introduction

The measurement of production cross-section of b -hadrons in pp or $p\bar{p}$ collisions provides an important test of perturbative quantum chromodynamics. A number of measurements have been performed at the Tevatron in $p\bar{p}$ collisions up to $\sqrt{s} = 1.96$ TeV and the latest results [1] are in good agreement with theoretical predictions. However, the evolution of the cross-section at higher energies is still affected by a large uncertainty and precise measurements are needed. This note presents the measurement of B^0 mesons production cross-section in pp collisions at $\sqrt{s} = 7$ TeV at the Large Hadron Collider (LHC). It is performed with the LHCb detector in the pseudorapidity interval $2 < \eta < 6$, with an integrated luminosity of 14.9 nb^{-1} .

Among the exclusive b -hadron decays, the semi-leptonic modes have the highest branching ratio and are well-suited for a cross-section measurement from the first LHC data. The reconstruction of exclusive decays with missing mass due to the neutrino is a difficult task at hadronic colliders. However, the secondary vertex reconstruction and particle identification capabilities of the LHCb detector allow events to be selected with good efficiency and low background contamination.

Semi-leptonic decays of B^0 mesons² are reconstructed in the channel $B^0 \rightarrow D^{*-} \mu^+ \nu_\mu$ where the charm mesons are reconstructed respectively in the hadronic modes $D^{*-} \rightarrow \bar{D}^0 \pi^-$, $\bar{D}^0 \rightarrow K^+ \pi^-$. Final states with additional particles which are not explicitly reconstructed are also included. These are the decays into an orbitally excited charmed meson of higher mass $B^0 \rightarrow D^{**} \mu^+ \nu_\mu$ (where D^{**} indicate generically the states D_1 , D_2^* , D_0^* and D_1') followed by $D^{**} \rightarrow D^{*-} X$, decays to non resonant multi-pion states $B^0 \rightarrow D^{*-} (n\pi) \mu^+ \nu_\mu$, as well as the decay $B^0 \rightarrow D^{*-} \tau^+ \nu_\tau$ followed by $\tau^+ \rightarrow \mu^+ \nu_\mu \bar{\nu}_\tau$.

The cross-section for producing a B^0 or a \bar{B}^0 meson is defined as:

$$\sigma(pp \rightarrow B^0 X) = \frac{N(B^0 \rightarrow D^{*-} \mu^+ \nu_\mu X)}{\mathcal{L}_{int} \times \epsilon \times \mathcal{B}(B^0 \rightarrow D^{*-} \mu^+ \nu_\mu X)} \quad (1)$$

where $N(B^0 \rightarrow D^{*-} \mu^+ \nu_\mu X)$ is the number of observed decays in the considered mode, \mathcal{L}_{int} is the integrated luminosity, ϵ is the total efficiency for detecting the events and $\mathcal{B}(B^0 \rightarrow D^{*-} \mu^+ \nu_\mu X) = \mathcal{B}_{tot}^{vis} = (1.68 \pm 0.17) \times 10^{-3}$ is the total semi-inclusive branching fraction, corresponding to the sum of the exclusive and inclusive partial contributions listed in Table 1. The dominant contribution is taken from Ref [2]. For decays which involve an excited resonant or non resonant state decaying into $D^{*-} (n\pi)$ the values have been derived from the inclusive branching ratio determination using some assumptions that are discussed in detail in the Appendix. The error includes a systematical uncertainty that is assumed for the $D^{*-} (n\pi)$ modes, which contribute $\sim 15\%$ of the total branching ratio.

The B^0 mesons are required to have pseudorapidity $\eta = -\ln(\tan(\frac{\theta}{2}))$ in the interval $2 < \eta < 6$. The B^0 polar angle, θ , is defined as the angle between the spectrometer axis along the beams and the line from the primary (pp collision) to secondary (B decay) vertexes. Its reconstruction is not affected by the unmeasured neutrino.

The measured cross section is extrapolated to an inclusive b -hadron cross-section using an external measurement of the B^0 production fraction and to the full phase space using PYTHIA 6.421 [3] pp collision generator.

²Charged conjugate modes are implied throughout this paper.

Decay mode	\mathcal{B}	$\mathcal{B}^{vis} \times 10^3$
$B^0 \rightarrow D^{*-} \mu^+ \nu_\mu$	0.0516 ± 0.0011	1.359 ± 0.035
$B^0 \rightarrow D^{*-} \tau^+ \nu_\tau$	0.016 ± 0.005	0.073 ± 0.023
$B^0 \rightarrow (D^{*-} n\pi) \mu^+ \nu_\mu$	0.0093 ± 0.0009	0.245 ± 0.024
$\tau^+ \rightarrow \mu^+ \nu_\mu \bar{\nu}_\tau$	0.1736 ± 0.0005	
$D^{*-} \rightarrow \bar{D}^0 \pi^-$	0.677 ± 0.005	
$\bar{D}^0 \rightarrow K^+ \pi^-$	0.0389 ± 0.0005	

Table 1: Branching fractions for the decay modes of interest [2]. Contributions to \mathcal{B}^{vis} (see text for definition) are listed in the last column. The detailed derivation of the values for $B^0 \rightarrow (D^{*-} n\pi) \mu^+ \nu_\mu$ is given in the appendix.

2 Data selection

The data sample derives from the early period of the 2010 LHC run at $\sqrt{s}=7$ TeV. The LHCb detector is a forward spectrometer described in detail elsewhere [4].

The analysis uses different muon and hadron High Level Trigger (HLT) lines, based on the first level (L0) single muon or single hadron trigger decisions. The L0 single muon trigger selects one muon candidate with a transverse momentum p_T^μ larger than 320 MeV/c. The L0 hadron trigger selects hadrons with a transverse energy E_T^h larger than 1220 MeV/c. The HLT trigger lines, first confirm the L0 trigger decision, then refine the selection applying harder cuts on the triggering candidate or adding requirements to the rest of the event. The logical OR of five lines is used.

The first HLT1 muon line considered here applies a harder cut on the muon p_T^μ at 1.3 GeV/c. A second HLT1 muon line requires p_T^μ greater than 0.8 GeV/c but adds a requirement on the muon impact parameter (IP) with respect to the primary vertex to be greater than 80 μm . The HLT1 hadron lines select events either with one hadron L0 candidate or with two hadrons with similar requirements to the muon ones. The fifth line selects events with a muon candidate and a second track with a distance of closest approach smaller than 2 mm.

Fully-simulated Monte Carlo (MC) samples of signal and background events have been used to optimize the signal reconstruction, to determine the selection efficiencies and to perform background studies, as described below. Proton beam collisions are generated with PYTHIA (version 6.421) [3] and decays of hadronic particles are provided by EVTGEN (version 9.2) [5]. The generated particles are traced through the detector with GEANT4 [6], taking into account the details of the geometry and material composition of the detector.

The event selection is designed to select the decay chain $B^0 \rightarrow D^{*-} \mu^+ \nu_\mu X$, $D^{*-} \rightarrow \bar{D}^0 \pi^-$, $\bar{D}^0 \rightarrow K^+ \pi^-$, where X denotes all possible missing particles. Charged tracks used in B^0 reconstruction are required to be detected in the vertex detector and the tracking stations behind the magnet.

A \bar{D}^0 candidate is reconstructed by combining a pion and a kaon of opposite charge that originate from a common vertex. To identify the hadrons, the information from the Ring Imaging Cherenkov detector (RICH) [4] is exploited. Likelihoods for the kaon and pion hypotheses are calculated from the reconstruction of the Cherenkov rings in the RICH focal plane. To identify a particle as a kaon, the difference of the logarithm of the

likelihood for the kaon hypothesis and the pion hypothesis is required to be larger than zero ($\Delta \ln \mathcal{L}_{K\pi} > 0$). For the pion identification no additional requirement is made on the particle identification (PID). In order to reject badly reconstructed tracks, the track $\chi^2/d.o.f$ is required to be smaller than 5. Both particles are required to have a momentum larger than 2 GeV/c and a transverse momentum larger than 400 MeV/c. The impact parameter of the particles is calculated with respect to the reconstructed primary vertex (PV) [7]. In cases where more than one PV is found, the PV with respect to which the B^0 has the smallest impact parameter significance is used. To suppress the background the IP is required to be larger than 50 μm and the χ^2 formed by using the hypothesis that the IP is equal to zero, χ_{IP}^2 , to be larger than 4. The $K\pi$ vertex is required to have a $\chi^2/d.o.f$ smaller than 10 and an invariant mass within 60 MeV/c² of the nominal \bar{D}^0 mass. The mass resolution from a simple Gaussian fit is 10.3 MeV/c².

To make a D^{*-} , the \bar{D}^0 candidate is combined with a track of the same charge as the pion from the \bar{D}^0 . This pion is called the “slow pion” π_{sl} below. No PID requirement is made on π_{sl} , but the track $\chi^2/d.o.f$ is required to be smaller than 5, the transverse momentum has to be larger than 110 MeV/c and the impact parameter with respect to the PV is required to be larger than 40 μm . The \bar{D}^0 and the π_{sl} are fitted to a vertex which is required to have a $\chi^2/d.o.f$ smaller than 15 and a mass within 80 MeV/c² of the nominal D^{*-} mass. The mass difference $\Delta m = m(\bar{D}^0\pi_{sl}^-) - m(\bar{D}^0)$ is required to be in the range 140.0–165.5 MeV/c².

To reconstruct the B^0 , the D^{*-} candidate is combined with a particle of the opposite charge (RS) which has been identified as a muon. The muon identification is based on the number of hits in the muon chambers associated to the track and on the global likelihood for the muon hypothesis with respect to the pion one. The difference of the logarithm of the likelihood for the muon hypothesis and the pion hypothesis is required to be greater than -4 ($\Delta \ln \mathcal{L}_{\mu\pi} > -4$). The muon is required to have momentum larger than 3 GeV/c, the transverse momentum larger than 800 MeV/c and the track $\chi^2/d.o.f$ smaller than 5. In addition, it is required that the muon impact parameter with respect to the primary vertex be larger than 40 μm with a χ_{IP}^2 larger than 4.

The fitted \bar{D}^0 and muon vertex is required to have a $\chi^2/d.o.f$ smaller than 15. The B^0 candidate is required to have an invariant mass in the range 3000–5220 MeV/c². The B^0 candidate is also required to point to the PV: the angle, $\delta\theta_B$, between the momentum of the candidate and the direction of flight is required to be smaller than 44.7 mrad. The direction of flight is determined from the position of the PV and the decay vertex. The difference between the z -coordinate of the B^0 vertex and that of the \bar{D}^0 vertex is required to be larger than -2.5 mm.

The complete list of selection requirements applied to the \bar{D}^0 , D^{*-} and B^0 candidates are reported in Table 2.

The same criteria described above, but with opposite D^* and muon charge correlation, are used to select a sample of wrong sign (WS) combinations $D^{*\pm}\mu^\pm$. This sample is used for background cross checks. The corresponding two dimensional mass distributions are shown in Figure 1.

The \bar{D}^0 and D^{*-} selection criteria are also used to obtain an inclusive D^{*-} sample with larger statistics than those of the B^0 sample. This sample is used to study the D^{*-} reconstruction properties, both in the mass and in the \bar{D}^0 impact parameter distributions. In order to reduce the larger background seen in the absence of any requirement on the presence of the muon, the \bar{D}^0 from D^{*-} candidates are required in addition to point to

D^0 selection cuts		D^{*-} selection cuts	
Variable	selection cut	Variable	selection cut
track $\chi^2/d.o.f (K^+, \pi^-)$	< 5	track $\chi^2/d.o.f (\pi_{sl}^-)$	< 5
K^+ PID	$\Delta \ln \mathcal{L}_{K\pi} > 0$		
$p(K^+, \pi^-)$	$> 2 \text{ GeV}/c$		
$p_T (K^+, \pi^-)$	$> 0.4 \text{ GeV}/c$	$p_T (\pi_{sl}^-)$	$> 110 \text{ MeV}/c$
$IP_{PV}(K^+, \pi^-)$	$> 0.05 \text{ mm}$	$IP_{PV}(\pi_{sl}^-)$	$> 0.04 \text{ mm}$
$\chi_{IP}^2(K^+\pi^-)$	> 4		
vertex $\chi^2/d.o.f (K^+\pi^-)$	< 10	vertex $\chi^2/d.o.f (\bar{D}^0\pi_{sl}^-)$	< 15
$p_T (\bar{D}^0)$	$> 1.6 \text{ GeV}/c$		
Flight $\chi^2(\bar{D}^0)$	> 50		
$ m(K^+\pi^-) - m(\bar{D}^0_{PDG}) $	$< 60 \text{ MeV}/c^2$	$ m(\bar{D}^0\pi_{sl}^-) - m(D_{PDG}^{*-}) $	$< 80 \text{ MeV}/c^2$
		$m(\bar{D}^0\pi_{sl}^-) - m(\bar{D}^0)$	$140. - 165.5 \text{ MeV}/c^2$

B^0 selection cuts	
Variable	selection cut
track $\chi^2/d.o.f (\mu^+)$	< 5
μ^+ PID	$\Delta \ln \mathcal{L}_{\mu\pi} > -4.0$
$p_T (\mu^+)$	$> 800 \text{ MeV}/c$
$IP_{PV}(\mu^+)$	$> 0.04 \text{ mm}$
$\chi_{IP}^2(\mu^+)$	> 4
vertex $\chi^2/d.o.f (D^{*-}\mu^+)$	< 6.6
$ \delta\theta_B $	$< 44.7 \text{ mrad}$
$z(\bar{D}^0) - z(B^0)$	$> -2.5 \text{ mm}$
$m(D^{*-}\mu^+)$	$3.0\text{-}5.2 \text{ GeV}/c^2$

Table 2: Cuts applied to select \bar{D}^0 , D^{*-} and signal B^0 candidates.

the PV with a pointing angle smaller than 66.3 mrad. As a consequence of this cut the sample is enriched in prompt D^{*-} candidates.

3 Luminosity

The absolute luminosity was measured at specific periods during the data-taking using both van der Meer scans and the ‘beam-profile’ method [8]. Two van der Meer scans were performed in a single fill of the LHC. Analysis of these scans yielded consistent results for the absolute luminosity scale with a precision of around 10%, dominated by uncertainty in the knowledge of the beam currents. In the second approach, six separate periods of stable running were chosen, and the beam-profiles were measured using beam-gas and beam-beam interactions. Using these results, correcting for crossing angle effects, and knowing the beam currents, it was possible to determine the luminosity in each period following the analysis procedure described in [9]. Consistent results were found for the absolute luminosity scale in each period, with a precision of 10%, which is again dominated by the uncertainty in the knowledge of the beam currents. The result agrees with the van der Meer analysis.

The knowledge of the absolute luminosity scale was used to calibrate counters which enabled the integrated luminosity to be calculated for each file of data used in the analysis.

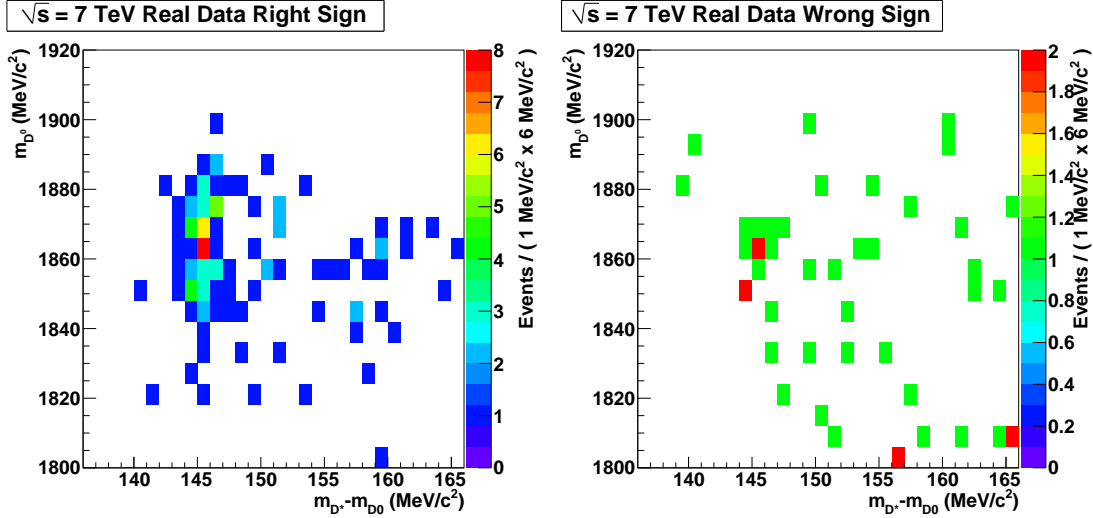


Figure 1: Two dimensional distribution of the D^0 mass versus the mass difference of D^* and D^0 for the $B^0 \rightarrow D^{*-} \mu^+ \nu_\mu$ candidates with the right charge muon and D^* combination (left) and with the wrong charge combination (right).

The counter used in this analysis was the number of hits recorded in the Scintillator Pad Detector (SPD) system [4]. During data-taking the SPD system was sampled randomly at a rate of 1 kHz. The detector response was stable throughout the data-taking period.

The integrated luminosity for the runs considered in this analysis was determined to be $14.9 \pm 1.5 \text{ nb}^{-1}$.

4 Signal yield determination

The determination of the number of $B^0 \rightarrow D^{*-} \mu^+ \nu_\mu X$ signal events is performed in three steps.

First the number of $D^{*-} \mu^+$ candidates, $N(D^* \mu)$, is extracted with an unbinned maximum likelihood fit to the two-dimensional distribution of the invariant mass $m(\bar{D}^0)$ and the difference of the invariant masses $\Delta m = m(\bar{D}^0 \pi_{sl}^-) - m(\bar{D}^0)$. The signal is described by a single Gaussian peaking at the \bar{D}^0 mass and by a double Gaussian for Δm . The background is described by two components, to account for candidates with or without a true \bar{D}^0 , respectively. The result of the fit is shown in Figure 2 and gives $N(D^* \mu) = 65 \pm 9$ events.

These events come from $b\bar{b}$ and $c\bar{c}$ production:

$$N(D^* \mu) = N(D^* \mu)_b + N(D^* \mu)_c. \quad (2)$$

To disentangle these two contributions an unbinned maximum likelihood fit to the \bar{D}^0 impact parameter distribution is performed. Background under the \bar{D}^0 and D^* mass peaks is subtracted using the sWeight procedure [10], with the weights determined using the previous fit to the mass distributions.

The shape of the $b\bar{b}$ component is modelled on simulated MC signal events while the shape of the $c\bar{c}$ component is determined from the inclusive D^* sample described in

Section 2. In both cases the distribution of the logarithm of the \bar{D}^0 IP is well described by a bifurcated Gaussian. The fit results are shown in Figure 3 and give $N(D^*\mu)_b = 50 \pm 8$ and $N(D^*\mu)_c = 15 \pm 5$.

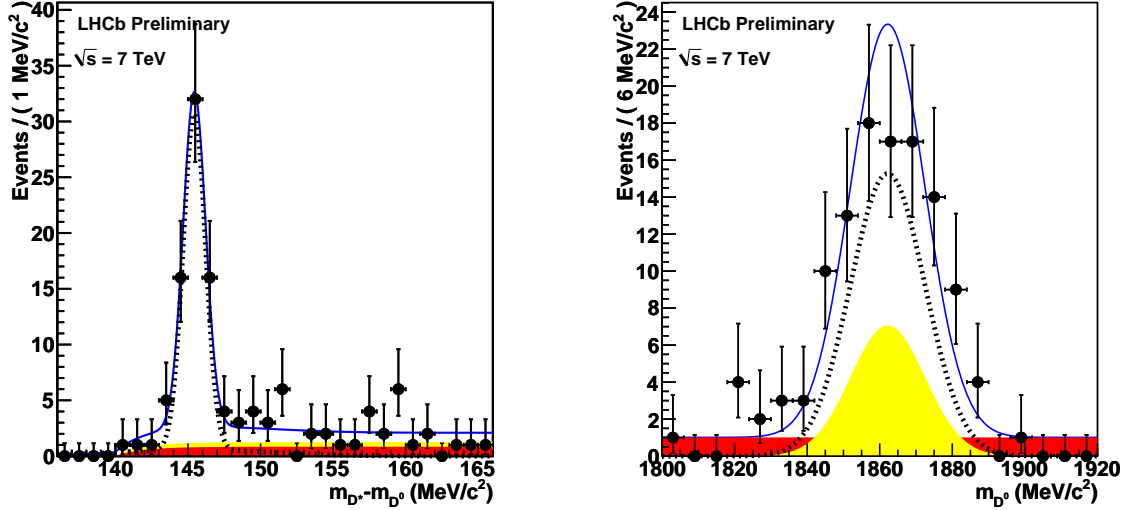


Figure 2: Results of the unbinned maximum likelihood fit to the two-dimensional mass distribution of the $B^0 \rightarrow D^{*-}\mu^+\nu_\mu$ candidates. Left and right plots show the projections of the mass difference Δm and of the invariant mass $m(\bar{D}^0)$, respectively. The data are represented by points with error bars. The fit results are superimposed (blue solid line). The $D^{*-}\mu^+$ signal contribution is shown by the black dotted line. The background containing a true D^0 is shown in yellow. Fake D^0 combinations are shown in red.

Finally the number of signal events is determined by applying a correction for the expected fraction, f_b , of $b\bar{b}$ background events in the selected sample:

$$N(B^0 \rightarrow D^{*-}\mu^+\nu_\mu X) = N(D^*\mu)_b(1 - f_b), \quad (3)$$

The fraction f_b is estimated from MC. The main contribution to this arises from B^+ mesons decaying into the same set of particles as the signal, plus one or more tracks: $B^+ \rightarrow D^{*-}\mu^+\nu_\mu X^+$. This gives $f_{B^+} = 0.102 \pm 0.012$, compatible with the ratio of branching ratios of B^+ and B^0 in the considered decay mode. Another contribution to f_b is due to combinations of a true D^{*-} and a true muon not directly originating from the same meson and is determined to be: $f_{b-\mu} = 0.045 \pm 0.008$. Thanks to the excellent muon identification performance of the detector ($\epsilon_{\pi \rightarrow \mu} \sim 2.3\%$), the background due to fake combination of true D^{*-} and a track misidentified as a muon is small and it is estimated to be $f_{b-misID} = 0.020 \pm 0.005$. Summing the different terms f_b is obtained: $f_b = f_{B^+} + f_{b-misID} + f_{b-\mu} = 0.167 \pm 0.016$, where the error quoted is due to the MC statistics. The systematic error on this quantity will be discussed in Section 6.

Several cross checks on the procedure used for signal extraction have been performed, as described below. The procedure has been applied to a sample of fully simulated inclusive D^* events, obtaining a good agreement between the result and the true number of signal events.

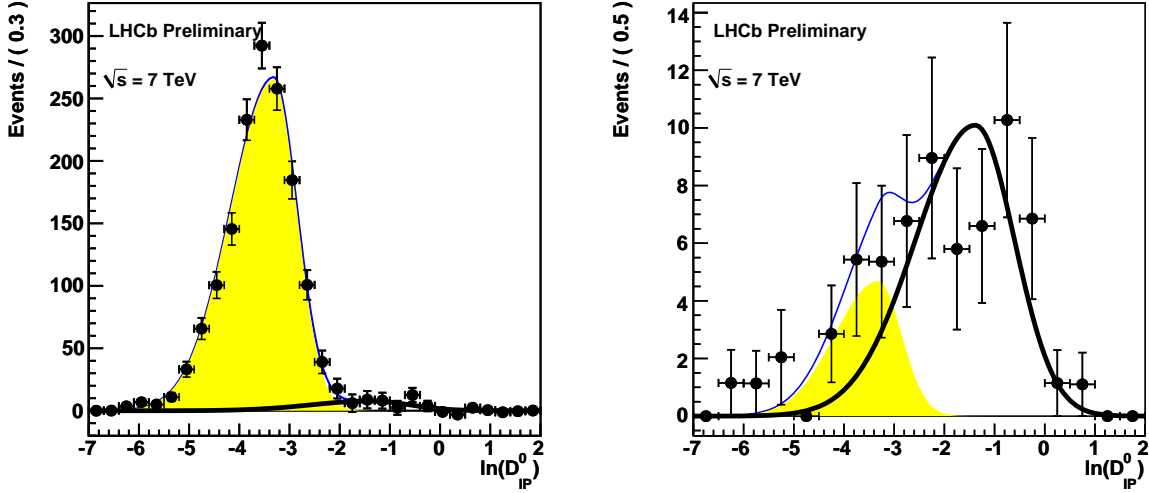


Figure 3: Results of the simultaneous fit to the distribution of $\ln(D_{IP}^0)$ of the data samples selected with the inclusive D^* (left) and $B^0 \rightarrow D^{*-} \mu^+ \nu_\mu$ selections (right). The weighted data are represented by points with error bars. The fit results are superimposed (blue solid line). The $b\bar{b}$ contribution is shown in black, the $c\bar{c}$ background contribution in yellow.

The full fit procedure has been applied to the selected sample of wrong sign combinations $D^{*\pm} \mu^\pm$, shown in Figure 1, for a cross check on the background containing a true D^{*-} . The mass fit gives: $N^{WS}(D^* \mu) = 11.2 \pm 3.7$ and is shown in Figure 4.

The fit to the distribution of the \bar{D}^0 meson impact parameter, shown in Figure 5, gives: $N_b^{WS} = 3.2 \pm 3.0$ events and $N_c^{WS} = 7.7 \pm 2.8$ events. These numbers compare well with those obtained using the ratio of wrong sign to right sign combinations of true D^{*-} expected from the simulation: $N_b^{WS,exp} = 1.5 \pm 0.4$ and $N_c^{WS,exp} = 4.7 \pm 1.9$.

A simplified fitting procedure has been developed in order to cross check the analysis described above. This does not rely on the use of sWeights. A fit to the $\ln(D_{IP}^0)$ distribution of all $D^* \mu$ events in a $\pm 5 \text{ MeV}/c^2$ window around Δm and a four-sigma window around the nominal D^0 mass is performed. The fit model is constructed using identical prompt and secondary components as in the standard procedure, but adding a third component for background events that sit under the Δm peak. The parameters for the $\ln(D_{IP}^0)$ background distribution have been fitted in the high sideband ($\Delta m > 150.45 \text{ MeV}/c^2$) region. This fit yields results compatible with the full procedure.

5 Efficiency determination

The total efficiency ϵ for detecting the events is determined as the product of three independent terms:

$$\epsilon = \epsilon_{sel} \times \epsilon_{gen} \times \epsilon_{trig}, \quad (4)$$

where ϵ_{sel} is the efficiency to reconstruct and select a signal event with the B^0 meson pseudorapidity in the interval $2 < \eta < 6$; ϵ_{gen} accounts for the MC generation cuts that

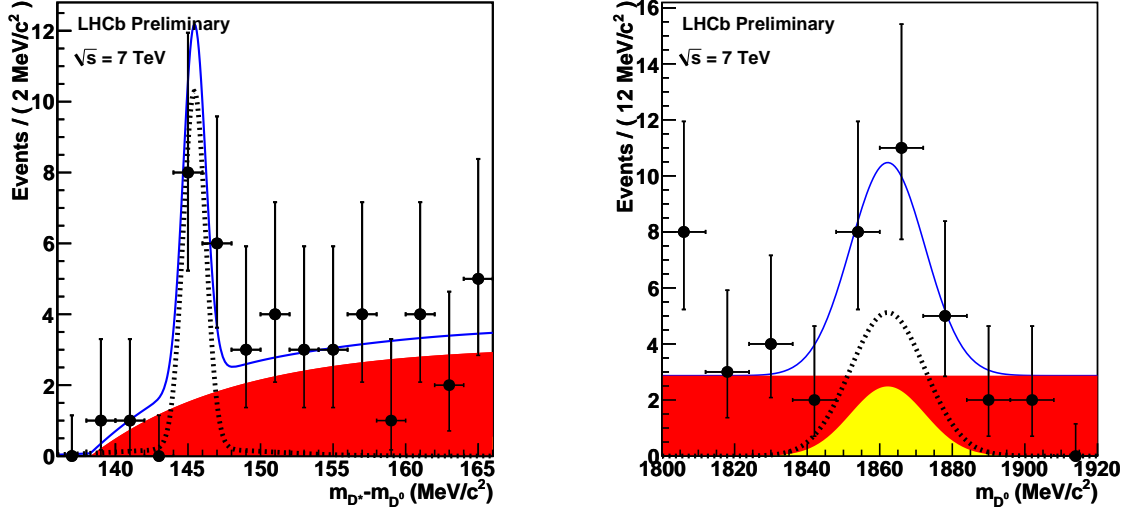


Figure 4: Results of the unbinned maximum likelihood fit to the two-dimensional mass distribution of the wrong charge combinations $D^{*\pm}\mu^{\pm}$. Left and right plots show the projections of the mass difference $\Delta m = m(\bar{D}^0\pi_{sl}^-) - m(\bar{D}^0)$ and of the invariant mass $m(\bar{D}^0)$ respectively. Superimposed to the data (black points with errors) is the total best fit function (blue solid line), separated in its partial contributions: signal (black dotted line), peaked background (yellow) and flat background (red).

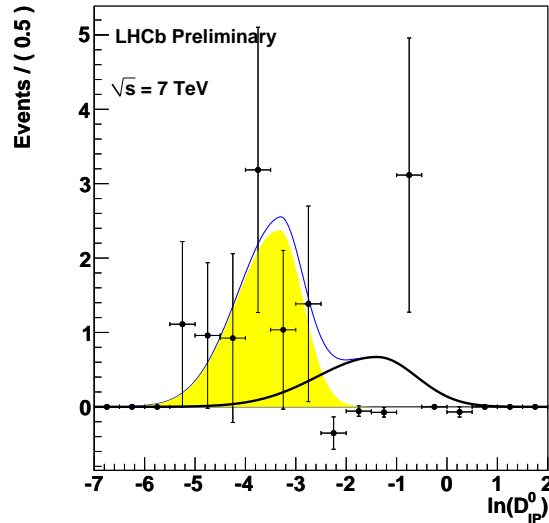


Figure 5: Results of the fit to the distribution of $\ln(D_{IP}^0)$ of the charge combinations $D^{*\pm}\mu^{\pm}$ in the data. The weighted data are represented by points with error bars. The fit results are superimposed (blue thin line). The $b\bar{b}$ contribution is shown in black, the $c\bar{c}$ background contribution in yellow (gray).

are applied in order to speed up the simulation³ and ϵ_{trig} is the efficiency for triggering on a selected and reconstructed signal event.

The selection efficiency is determined by fitting the signal MC data: $\epsilon_{sel} = 0.0506 \pm 0.0005$ (fit error only).

Possible differences in the efficiency of the particle identification requirements in data with respect to the simulation have been considered. For kaon identification, a separate study has been performed by using calibration samples of $\phi \rightarrow K^+ K^-$ decays, as described in Ref. [11]. The efficiency for the selection cuts used in this analysis has been evaluated convolving these results, which are determined in bins of η and p_T , with the spectra of the kaon candidates. It was compared to that derived from the MC simulation and a correction factor of $0.984 \pm 0.005 \pm 0.018$ was determined, where the first error is statistical and the second reflects possible differences in the kaon spectra in data with respect to the MC simulation. The comparison of efficiencies in data and MC for the muon identification, as a function of muon momentum was performed on a sample of $J/\psi \rightarrow \mu^+ \mu^-$ events. These efficiencies agree at the 2.5% level [12]. Therefore no correction is applied but a systematic uncertainty of 2.5% is assigned.

The generation efficiency was determined using PYTHIA 6.421 [3]. The ratio between the number of generated B^0 mesons in the interval $2 < \eta < 6$ with tracks in the LHCb acceptance and the total number of generated B^0 mesons in the interval $2 < \eta < 6$ is: $\epsilon_{gen}^{2 < \eta < 6} = 0.605 \pm 0.002$. In order to calculate a cross-section for the production of B^0 mesons in 4π the generator efficiency with respect to B^0 mesons generated in the full rapidity range is also calculated: $\epsilon_{gen}^{4\pi} = 0.1606 \pm 0.0006$.

The efficiency for triggering the events by any of the five selected HLT1 lines was measured on MC events to be $\epsilon_{trig} = 0.939 \pm 0.002$ (statistical error only). Since a combination of different trigger lines was used, both with and without muon requirement, and with and without impact parameter cuts, the triggering scheme has a built in redundancy. To check the consistency between data and MC the procedure of signal extraction was repeated for two sub-samples of events. Those samples used only the hadron lines or only the muon lines respectively. The efficiency-corrected number of signal events was found to be compatible to the one obtained from the full sample. As a consequence the efficiency obtained from the simulation is used and a systematic uncertainty of 10% assigned to the trigger efficiency.

6 Systematic studies

The main systematic uncertainties on the B^0 production cross-section are related to the luminosity measurement, to the tracking efficiency, to the visible branching ratio and to the trigger efficiency. The list of all systematic uncertainties is summarized in Table 3; some of these have been discussed in previous sections.

For the uncertainty in the track reconstruction efficiency, we rely on independent studies [13] which demonstrate that data and MC efficiencies are in agreement at a level of 3% for the D^0 decay products and 4% for the muon and the slow pion. This uncertainty is conservatively assumed to be uncorrelated among the four tracks of the B^0 decay, giving a total systematic of 14%.

³The signal MC sample contains events in which the both the D^0 products and the muon are required to match the nominal LHCb detector acceptance: $0.010 < \theta < 0.400$ rad

The uncertainty on the selection efficiency has a contribution due to different exclusive and inclusive contributions to the signal BR which amounts to 2.5%. This variation should be partially compensated by the systematic effects on the visible BR, but the correlation was conservatively neglected and a total systematic uncertainty on the selection efficiency of 2.7% was assigned.

The uncertainty related to the subtraction of the residual $b\bar{b}$ background has been estimated for each contribution separately, as the quadratic sum of the statistical uncertainty of the MC and the systematic effects. For the B^+ background an additional systematic uncertainty was evaluated from the variation of the assumed branching fraction, using assumptions similar to the B^0 case, and a total uncertainty of 7% was determined. For the contribution due to misidentified muons and true D^* , considering a variation of the mis-identification probability in data with respect of the simulation of 10%, a total uncertainty of 0.5% is obtained. For the contribution of combination of true D^* and true muons coming from different sources, assuming a variation of the background sources in the MC of 50% a 2.4% uncertainty is obtained.

The uncertainty related to the visible branching fraction has been estimated using the values in Table 1 and taking into account the variation of the assumptions made to calculate the contribution due to the semi-inclusive decays, as discussed in the appendix.

Source	Uncertainty (%)
luminosity	10
tracking efficiency	14
selection efficiency	2.7
kaon ID	1.8
muon ID	2.5
$b\bar{b}$ background subtraction due to μ mis-ID	0.5
$b\bar{b}$ background subtraction due to true μ combinations	2.4
$b\bar{b}$ background subtraction due to B^+	7
trigger efficiency	10
visible branching fraction	10
Total	24

Table 3: Relative systematic uncertainties on the measured B^0 cross-section.

7 Cross-section determination

Using Equation (1) the cross-section for producing a B^0 or a \bar{B}^0 meson, in the pseudorapidity interval $2 < \eta < 6$ is determined to be:

$$\sigma(pp \rightarrow B^0 X, 2 < \eta(B^0) < 6) = 59 \pm 9 \pm 14 \mu\text{b}, \quad (5)$$

where the first error is statistical and the second is systematic.

From this measurement, an inclusive b -hadron cross section can also be derived, by using the external measurement of the B^0 fraction performed at LEP [14]. The value of the b -hadron fractions was obtained analyzing an unbiased sample of weakly decaying b -hadrons produced at high energy, with the B^0 and the B^+ mesons assumed to be produced

in equal amount: $f(B^0) = f(B^+) = 0.403 \pm 0.009$. To account for possible differences of these fractions in high energy hadronic collisions with respect to those at LEP in Z decays, the Tevatron result (0.333 ± 0.030) [14] is also considered:

$$\sigma(pp \rightarrow b\bar{b}X, 2 < \eta(b\text{-hadron}) < 6) = 73 \pm 12 \pm 17 \mu\text{b}, \text{ using } f(B^0) \text{ from LEP} \quad (6)$$

$$\sigma(pp \rightarrow b\bar{b}X, 2 < \eta(b\text{-hadron}) < 6) = 89 \pm 14 \pm 21 \mu\text{b}, \text{ using } f(B^0) \text{ from Tevatron} \quad (7)$$

where the first error is statistical and the second is systematic. These results are in agreement with the prediction of $\sigma^{th}(pp \rightarrow b\bar{b}X, 2 < \eta(B^0) < 6) = 70_{-27}^{+31} \mu\text{b}$ of Ref. [15].

Using the generation efficiency $\epsilon_{gen}^{4\pi}$ from Section 5, the cross-section for b -hadron production in the full phase space can be obtained:

$$\sigma(pp \rightarrow b\bar{b}X) = 275 \pm 44 \pm 66 \mu\text{b}, \text{ using } f(B^0) \text{ from LEP} \quad (8)$$

$$\sigma(pp \rightarrow b\bar{b}X) = 333 \pm 53 \pm 80 \mu\text{b}, \text{ using } f(B^0) \text{ from Tevatron} \quad (9)$$

where, again, the first error is statistical and the second is systematic. As a reference the value in the simulation (PYTHIA 6.421 and EVTGEN) is $\sigma_{Pythia}^{4\pi}(pp \rightarrow b\bar{b}X) = 457 \pm 48 \mu\text{b}$.

The same quantity was measured by LHCb studying other two b -hadron decay channels: $J/\psi X$ [12] and $D^0 \mu X$ [16]. In the first case, by analyzing the time distribution of the reconstructed J/ψ decaying to muon pairs it was possible to determine the rate of b -hadron decays. In the second case, the B^0 is partially reconstructed using the decay products $D^0 \rightarrow K^+ \pi^-$ and μ . The corresponding results, calculated with the LEP hadronization factor are respectively: $\sigma_{J/\psi X}^{4\pi}(pp \rightarrow b\bar{b}X) = 319 \pm 24 \pm 59 \mu\text{b}$ and $\sigma_{D^0 \mu X}^{4\pi}(pp \rightarrow b\bar{b}X) = 292 \pm 15 \pm 43 \mu\text{b}$, in good agreement with the results obtained from the present analysis.

8 Conclusion

The measurement of B^0 meson production cross-section in pp collisions at $\sqrt{s} = 7$ TeV in the pseudorapidity interval $2 < \eta < 6$ has been performed with the LHCb detector at LHC. Semi-leptonic decays $B^0 \rightarrow D^{*-} \mu^+ \nu_\mu X$, $D^{*-} \rightarrow \bar{D}^0 \pi^-$, $\bar{D}^0 \rightarrow K^+ \pi^-$ were reconstructed from 14.9 nb^{-1} of data. The result is used to derive the inclusive b -hadron production cross-section in the same pseudorapidity interval and is extrapolated to the full phase space. The above results are in good agreement with those obtained from b decays into $D^0 \mu \nu X$ [16] and $J/\psi X$ [12] and with the theoretical predictions [15].

9 Appendix

The determination of the visible branching ratio (\mathcal{B}^{vis}) of the semi-leptonic decay $B^0 \rightarrow D^{*-} \mu^+ \nu_\mu X$ is obtained by adding the contributions of several terms.

The main contributions are the exclusive decays $B^0 \rightarrow D^{*-} l^+ \nu_l$, with the lepton being either a muon or a tau, whose branching ratios (BR) are measured directly. Combining the values of Ref. [2], quoted as Γ_6 and Γ_7 with the BR for the decays $D^{*-} \rightarrow \bar{D}^0 \pi^-$, $\bar{D}^0 \rightarrow K^+ \pi^-$ and $\tau^+ \rightarrow \mu^+ \nu_\mu \bar{\nu}_\tau$ the values: $\mathcal{B}^{vis}(B^0 \rightarrow D^{*-} \mu^+ \nu_\mu) = (1.359 \pm 0.035) \times 10^{-3}$ and $\mathcal{B}^{vis}(B^0 \rightarrow D^{*-} \tau^+ \nu_\tau) = (0.073 \pm 0.023) \times 10^{-3}$ are determined, respectively. Additional

contributions come from decays with intermediate orbitally excited resonant D^{**} state (generic name for the states D_1 , D_2^* , D_0^* and D_1') followed by $D^{**} \rightarrow D^{*-}X$ and from non resonant decays to $D^*n\pi$. Their amounts are related to the measurement of the BR of inclusive decay $B^0 \rightarrow (D^{(*)}n\pi)^-\mu^+\nu_\mu$: $\Gamma_{11}=(2.4\pm 0.5)\times 10^{-2}$. The same quantity can also be determined by combining the independent measurements of the total semi-leptonic inclusive BR, $B^0 \rightarrow l^+\nu_l X$ (Γ_1), the exclusive ones, $B^0 \rightarrow D^-l^+\nu_l$ (Γ_4) and $B^0 \rightarrow D^{*-}l^+\nu_l$ (Γ_6) and the fraction of $b \rightarrow u$ transitions derived from the B^0 mixing (Γ_{bu}) as given in Table 4:

$$\mathcal{B}(B^0 \rightarrow (D^{(*)}n\pi)^-\mu^+\nu_\mu) = \Gamma_1 - \Gamma_4 - \Gamma_6 - \Gamma_{bu} = (2.77 \pm 0.32) \times 10^{-2}. \quad (10)$$

Channel	Branching ratio
Γ_1	$(10.33\pm 0.28)\times 10^{-2}$
Γ_4	$(2.17\pm 0.12)\times 10^{-2}$
Γ_6	$(5.16\pm 0.11)\times 10^{-2}$
Γ_{bu}	$(0.23\pm 0.02)\times 10^{-2}$

Table 4: Branching ratios from [2]. Definitions are given in the text.

Given the compatibility of this value with the independent measurement Γ_{11} the average value $=(2.66\pm 0.26)\times 10^{-2}$ is used here.

This BR is multiplied by two factors: F_1 expressing a fraction of this rate which produces D^* resonances, and F_2 expressing the fraction of D^* 's which are charged. Assuming that larger pion multiplicities equalize the amount of charged and neutral D^* the value $F_2=1/2$ is used. $F_1=0.7$ is used, based on $\mathcal{B}(B^0 \rightarrow D^{*-}\mu^+\nu_\mu)/\mathcal{B}(B^0 \rightarrow D^-\mu^+\nu_\mu)=2.38$ [2]. There is a considerable uncertainty in F_1 , since the value is based on weak hadronic current coupling of the B^0 to D^* or D , whereas F_1 has to do with strong interactions mediating pion transitions between various excitations of D meson system. F_1 may vary considerably from one D^{**} resonance to other, as evidenced by the measurements: $F_1=0.34\pm 0.13$ for $D_2^*(2460)^-$, $F_1 > 0.85$ for $D_1(2400)^+$ [2]. The non-resonant contributions to F_1 are also hard to predict. Therefore, a generous systematic uncertainty is considered, to cover both F_1 and F_2 uncertainties and $F_1 \times F_2=0.35\pm 0.22$ is used. This is a 63% relative uncertainty. As a result the total relative uncertainty on the $\mathcal{B}_{tot}^{vis}=(1.68\pm 0.17)\times 10^{-3}$ results of 10%.

References

- [1] T. Aaltonen et al. [The CDF Collaboration], Phys. Rev. D79, 092003 (2009); arXiv:0903.2403.
- [2] K. Nakamura et al. [The PDG Collaboration], Journal of Physics G 37, 075021 (2010).
- [3] T. Sjostrand, S. Mrenna and P. Skands, JHEP 0605 (2006) 026 [arXiv:hep-ph/0603175].
- [4] B. Adeva *et al.* [The LHCb Collaboration], ‘‘The LHCb Detector at the LHC’’ Journal of Instrumentation (JINST), 2008 3 S08005.

- [5] A. Ryd et al., “EvtGen: a Monte Carlo generator for B-physics”, Babar Analysis Document (BAD) 522 (2005),
D. J. Lange, Nucl. Instrum. Meth. A 462 (2001) 152.
- [6] S. Agostinelli et al. [GEANT4 Collaboration], Nucl. Instrum. Meth. A 506 (2003) 250.
- [7] M. Krasowski, M Kucharczyk, W Mnner, G Polok and M Witek, “Primary vertex reconstruction”, CERN-LHCb-2007-011.
- [8] M. Ferro-Luzzi, Nucl. Instrum. Meth. A 553 (2005) 338.
- [9] LHCb Collaboration ”Prompt K_S^0 production in pp collisions at $\sqrt{s} = 0.9$ TeV” accepted by PLB. <http://dx.doi.org/10.1016/j.physletb.2010.08.055>
- [10] M. Pivk, F. R. Le Diberder, “sPlot: a statistical tool to unfold data distributions” Nucl.Instrum.Meth.A555:356-369,2005 and arXiv:physics/0402083v3
- [11] A.Powell in ICHEP2010 Proceedings.
- [12] “Measurement of the J/ψ production cross-section at $\sqrt{s} = 7$ TeV in LHCb” LHCb-CONF-2010-010.
- [13] S.Borghini in ICHEP2010 Proceedings.
- [14] <http://www.slac.stanford.edu/xorg/hfag/semi/fpcp2009/home.shtml>: on-line update of E. Barberio et al., Averages of b -hadron and c -hadron Properties at the End of 2007,arXiv:0808.1297
- [15] Private communication from S. Frixione, M. L. Mangano, P. Nason, and G. Ridolfi. See also M. Cacciari, S. Frixione, M. L. Mangano, P. Nason and G. Ridolfi. JHEP 0407 (2004) 33.
- [16] CERN-PH-EP-2010-029